

~~RESTRICTED~~

RM E51L13

NACA RM E51L13

NACA

RESEARCH MEMORANDUM

CLASSIFICATION CANCELLED

ANALYSIS OF COOLANT-FLOW REQUIREMENTS FOR AN
IMPROVED, INTERNAL-STRUT-SUPPORTED,
AIR-COOLED TURBINE-ROTOR BLADE

By Wilson B. Schramm and Alfred J. Nachtigall

Lewis Flight Propulsion Laboratory
Cleveland, Ohio

CLASSIFICATION CHANGED

To ~~Confidential~~

By authority of ~~Leg. W. Cronley~~ Date 12/1/53.

CLASSIFIED DOCUMENT

This material contains information relating to the national defense of the United States within the meaning of the espionage laws, Title 18, U.S.C., Secs. 793 and 794, the transmission or revelation of which in any manner to unauthorized person is prohibited by law.

NATIONAL ADVISORY COMMITTEE
FOR AERONAUTICS

WASHINGTON

February 14, 1952

~~CONFIDENTIAL~~

SECURITY INFORMATION

~~RESTRICTED~~

~~CONFIDENTIAL~~
~~SECURITY INFORMATION~~

NATIONAL ADVISORY COMMITTEE FOR AERONAUTICS

RESEARCH MEMORANDUMANALYSIS OF COOLANT-FLOW REQUIREMENTS FOR AN IMPROVED,
INTERNAL-STRUT-SUPPORTED, AIR-COOLED TURBINE-
ROTOR BLADE

By Wilson B. Schramm and Alfred J. Nachtigall

SUMMARY

A new type of air-cooled turbine-rotor-blade design based on the principle of submerging the load-carrying element in cooling air within a thin high-temperature shell which is attached to the load-carrying element by means of spot-welding was analytically evaluated using measured sea-level-static engine operating conditions for a J33 turbojet engine. A typical spanwise effective gas temperature profile at the rated engine speed was used. Temperatures at various significant stations in the blade cross section for several spanwise stations were calculated for three coolant-flow ratios.

The results indicated that this new principle of blade design allows the load-carrying element, or internal supporting strut, to be operated at a considerably lower temperature than that of the enveloping shell. The temperature difference was over 200° F for a coolant-flow ratio of 0.01 and increased with coolant-flow ratio. For this coolant-flow ratio the temperature of the internal supporting strut was well below 900° F, which was over 200° F cooler than the shell in a comparable shell-supported blade. This temperature difference also increased with coolant-flow ratio. To achieve the same cooling effectiveness in the load-carrying element or shell of a shell-supported blade as obtained at 0.01 coolant-flow ratio on the strut of the internally supported blade required almost 2.5 times as much coolant flow.

Comparison of the relative strength of internally supported and shell-supported blades showed that the internally supported blade has considerably greater potentiality to withstand the increased stresses that may be anticipated in future engines. Based on stress-to-rupture properties for 17-22A(S) for 1000-hour blade life, the internally supported blade can be operated at a permissible stress of 75,000 pounds per square inch or about four times that of a comparable shell-supported

~~CONFIDENTIAL~~
~~SECURITY INFORMATION~~

blade with a coolant-flow ratio of 0.01 and an effective gas temperature of 1530° F. For an effective gas temperature of 2530° F the internally supported blade required less than half as much coolant flow as the shell-supported blade to maintain a permissible stress of 60,000 pounds per square inch.

It appeared that placing the load-carrying element of the blade within the coolant passage will permit the lowest coolant flow of any of the convection-cooled configurations that have been previously investigated.

INTRODUCTION

Analytical and experimental investigations of air-cooled turbine blades have shown that high cooling effectiveness can be achieved through augmented internal heat-transfer surface in the coolant passage (references 1 to 3). Cyclic endurance investigations of typical air-cooled rotor blades under severe operating conditions in a turbojet engine indicate that the cooling effectiveness obtained with acceptable coolant-flow rates is sufficient to permit substitution of noncritical steels for the high-temperature blade alloys that contain large quantities of scarce metals (reference 4). Further increases in over-all cooling effectiveness are desirable, however, to improve the reliability of the turbine and to provide for eventual improvements in the air-handling capacity and performance of the jet engine.

Analytical investigations of air-cooled turbojet-engine performance (references 5 and 6) have shown the desirability of minimizing the flow of cooling air bled from the engine compressor. An important factor in controlling the coolant-flow rate is the configuration of the internal coolant passage. In air-cooled blade designs previously investigated, the extended internal heat-transfer surfaces are inserted into the hollow shell which forms the blade profile. This shell, which is directly exposed to the hot gases, is also the load-carrying element of the blade; and to some extent it must support the internal parts in addition to its own centrifugal load. A more effective integration of the cooling and structural characteristics of a blade can be obtained by concentrating the load-carrying element in the central portion by means of a strut to which is attached a thin shell that performs the aerodynamic function of the blade. In the internal-strut-supported blade, the centrifugal load of the shell is transferred directly to the internal supporting strut; and at the same time the heat transfer into the load-carrying element is reduced because of the protection offered by the shell.

2444 Analytical investigations were made at the NACA Lewis laboratory to evaluate the cooling characteristics of an air-cooled turbine blade using an internal finned strut as the load-carrying element. The principal objectives of the investigation were to determine the probable influence of the shell on the stress distribution in the strut, to analyze in detail the internal-strut and shell temperature distributions for a suitable experimental blade configuration, and to compare the calculated cooling effectiveness of the internal-strut-supported blade with that of an equivalent shell-supported blade. The purpose of this report is to present the results of the investigation, to compare the coolant-flow requirements of the two configurations, and to show what advantages an air-cooled internal-strut-supported blade may have over an equivalent shell-supported air-cooled blade.

The investigation was made using static sea-level operating conditions from a representative turbojet engine wherever needed to determine heat-transfer parameters on the outside surface of the blade. The particular configuration of an internal-strut and shell combination used in the investigation had been arrived at from a preliminary unpublished investigation of several different configurations. The calculations for this configuration were made for three different coolant flows which covered the anticipated range of required coolant flows. Since the cooling characteristics of the internal-strut-supported-blade configuration are dependent to a considerable extent on the method used for structural attachment of the shell to the strut, the analytical results presented apply specifically to the spot-welded attachment specified in the mechanical design of this configuration. The results, however, are believed representative of this general principle of blade construction.

SYMBOLS

The following symbols are used in this report:

- H_i heat-transfer coefficient on internal coolant-passage surfaces,
Btu/(sec)(sq ft)(°F)
- H_f fictitious heat-transfer coefficient representing heat flow to
secondary fin, Btu/(sec)(sq ft)(°F)
- H_o heat-transfer coefficient on outside blade surface,
Btu/(sec)(sq ft)(°F)
- k_f thermal conductivity of fin metal, Btu/(sec)(sq ft)(°F/ft)
- L_f depth of secondary fin (ft)

$T_{a,e}$	effective cooling-air temperature ($^{\circ}\text{F}$)
T_B	blade temperature ($^{\circ}\text{F}$)
$T_{g,e}$	effective gas temperature ($^{\circ}\text{F}$)
w_a/w_g	coolant-flow ratio
x/b	dimensionless measure of distance along span of blade from base
τ_f	thickness of secondary fin (ft)
Φ	dimensionless cooling-effectiveness parameter
φ_f	$\sqrt{\frac{2 H_1}{k_f \tau_f}}$

2444

ANALYSIS

The general methods of cooling analysis employed in this investigation have been well established previously, and numerous references are available (for example, reference 7). The discussion of methods of analysis is therefore limited to particular deviations from established principles, where necessary, to accommodate new factors introduced by the internal-strut-supported-blade configuration.

Description of Internal-Strut-Supported-

Blade Configuration

A typical internal-strut-supported-blade configuration is illustrated in figures 1 and 2. The blade consists of a thin metal shell having the shape of the blade profile and its internal supporting strut which may or may not be integral with the rotor disk. The purpose of the shell is to direct the flow of gases in the desired manner so that the aerodynamic forces are transmitted to the load-carrying element. The internal supporting strut has the general shape of the blade section, though smaller, and has projections in the shape of primary fins to which the shell is attached. The secondary fins between the primary fins do not touch the shell and serve only as extended heat-transfer surface to augment cooling of the strut. The spaces between the shell and internal strut not taken up by the fins serve as cooling-air passages into which air is introduced at the base of the blade and allowed to

2444

escape from the open ends of the passages at the tip. At any spanwise station the cross-sectional area of the internal supporting strut must be sufficiently large to support the centrifugal load of the shell in addition to that of its own weight in the centrifugal field. Because the internal supporting strut thus becomes heavily loaded at the base, it is necessary to taper the internal supporting strut toward the blade tip where less metal is required to carry the load. An essential principle of the design is that the shell be attached to the strut by means of the primary structural fins at numerous stations along the span so that its centrifugal load is never concentrated. If the shell were attached to the strut at the tip only, the shell would be subject to high compressive stresses and transmission of the entire weight of the shell to the strut at the tip of the blade would result in excessive tensile stresses in the strut in the tip region. If the shell were attached only at the root of the blade, the shell would be subjected to the full tensile centrifugal stress. It is therefore essential to provide attachment at numerous stations along the blade span.

With such an arrangement it can be seen that no severe tensile loading is imposed on the shell, and that it can therefore be operated without failure at higher metal temperatures than a conventional blade of the same material. If desired, a corrosion-resistant high-temperature metal shell may be used with a noncritical metal strut, as was done for the experimental design analyzed, with a substantial saving in over-all usage of critical material when compared with a blade made entirely from critical alloys. To permit the use of noncritical materials in the internal supporting strut and turbine disk and to utilize the greater strength of these metals at lower temperatures, the internal supporting strut must be insulated as much as possible from the hot shell and the surrounding hot gases. This objective can be accomplished in a number of ways. The method of attaching the shell to the primary fins on the strut is an important factor in controlling the strut temperature. Although it is desirable to minimize the area of intimate thermal contact between the shell and the internal supporting strut in order to minimize heat flow to the strut, sufficient mechanical contact between the shell and internal supporting strut is necessary, however, to hold the shell in place in the centrifugal field. For the experimental design used as a basis for the analysis in this report, the use of spot welding was desirable from fabrication considerations; it also offered a means of reducing the area of intimate thermal contact between the shell and the primary fins to the minimum amount required to keep the shell in place. The number and spacing of spot welds was selected on the basis of experimentally determined strengths of spot welds between a thin sheet and the edge of a fin at the elevated temperatures anticipated for this application. Other factors in controlling the strut temperature are the thermal conductivity of the material in the primary fins and the ratio of fin width to depth, which should be as low as permitted by structural considerations. In addition to these factors, cooling air is passed through the spanwise passages formed by the space between adjacent

spanwise fins enclosed by the shell. The convective heat-transfer coefficient resulting from this flow cools the shell as well as the fins and the strut surface. Some of the heat conducted through the integral primary fin to the strut can be transferred to the cooling air by increasing the area of strut surface exposed to the cooling air. This increase in area is accomplished by adding secondary fins to the strut on the area between the primary fins supporting the shell. Because these secondary fins are shorter, they have no contact with the shell and thus transfer heat only from the strut to the cooling air.

Temperature Distribution Analysis in

Internal-Strut-Supported Blade

In order to determine the over-all cooling characteristics of the internal-strut-supported blade, it was necessary to analyze the spanwise temperature distribution in both shell and internal strut. Deviation from the normal procedure of analysis was necessary because of the complexity of the heat flow path between hot gas and cooling air in this configuration. The heat flow path involves numerous changes in conductive cross section, for example between the primary structural fins and the body of the internal strut, and also the added complication of the spot welds between the shell and the primary fins.

The actual blade configuration was therefore replaced by a model which permitted a one-dimensional analysis of a representative cross section of the strut and shell using the mean spanwise geometry (fig. 3(b)). At the start of the analysis the cooling-air temperature at the blade base was used because this was the only station at which the cooling-air temperature was initially known. From this initial analysis, the nondimensional cooling-effectiveness parameter

$$\phi = \frac{T_{g,e} - T_B}{T_{g,e} - T_{a,e}}$$

was determined at various points within the blade cross section, where

$T_{a,e}$ local spanwise effective cooling-air temperature

T_B local spanwise blade temperature at a point on the blade cross section

$T_{g,e}$ local spanwise effective gas temperature

Also determined from this initial analysis was the effective coolant-passage heat-transfer coefficient for the inside perimeter of the shell. This coefficient was a function of the conduction through the spot welds into the strut as well as the direct convection cooling of the shell.

The combined effective coolant-passage heat-transfer coefficient was then used to determine the spanwise variation of the local cooling-air temperature in a one-dimensional analysis with spanwise variation of the gas temperature according to a specified temperature profile. By assuming that the heat-transfer coefficients from the gas to the blade shell and from the internal coolant-passage surfaces to the cooling air are constant spanwise and that a mean spanwise geometry can be used as a constant for the entire span, the nondimensional cooling-effectiveness parameters previously determined for various points in the cross section were the same at all spanwise stations when referred to local spanwise gas and coolant temperatures. It was then possible to calculate the spanwise temperature distribution in the internal strut and shell at the various points of interest in the cross section from the cooling-air temperature distribution and a specified effective gas temperature distribution.

One-dimensional cross-sectional temperature distribution. - The internal-strut and coolant-passage configuration used in this investigation is illustrated for the blade root station in figure 2. Inasmuch as no attempt was made to analyze temperatures in the leading and trailing edges, the results of this analysis apply only to the midchord section of the blade. With the configuration illustrated in figure 2, however, large chordwise temperature gradients would not be expected to occur as a result of the deviations of the geometry in the leading and trailing edges from that of the representative section analyzed, because the coolant passages extend well into these regions. If appreciably higher temperatures were encountered in the leading and trailing edges, the midchord section would still be the most significant because of the shift of loads to the cooler portions of the internal supporting strut. Further experimental blade endurance investigations are required to verify the extent of stress redistribution from the shell to the internal supporting strut and within the strut under actual operating conditions.

For assumed constant heat-transfer coefficients and constant gas and cooling-air temperatures in a cross-sectional plane, it can be seen that A-A, B-B, and C-C are lines of symmetry about which the temperature distribution is symmetrical and that there is no heat flow across these lines so that the temperature gradient across them is zero. It is therefore permissible to analyze the temperatures of one section enclosed by these lines and assume it is representative of the cross section between D-D and E-E. Of course, it will not be representative of the leading- and trailing-edge sections of the blade. For this reason

measurements of blade geometry needed in the analysis, for example, cross-sectional coolant-passage area and wetted perimeter, were made on the central portion of the blade sections as shown between D-D and E-E of figure 2.

The representative section of the blade profile enclosed by A-A, B-B, and C-C is again shown in figure 3(a) in detail. The element between stations 2 and 3 represents the spanwise average of the areas of intimate thermal contact in the nuggets of all the spot welds between the shell and a primary fin. The secondary fin attached to the internal strut at stations 5 and 6 has no thermal or physical contact with the shell and is assumed to conduct heat from the strut only. The elements of the section were arranged as shown in figure 3(b) in order to permit a solution of the problem as one-dimensional heat conduction, with heat being added or withdrawn from the sides of the elements by convective coefficients. The element between stations 1 and 2 represents the segment of the shell between A-A and B-B. All the heat flowing in the representative section enters through this element by means of an outside heat-transfer coefficient H_o . Some of the heat is conducted directly through the shell and transferred to the cooling air. The rest of the heat is conducted parallel to the shell toward the primary fins, where it is conducted through the nuggets of the spot welds into the primary fins. As the heat is conducted along the primary fin from station 3 to 4 and into the elements of the internal supporting structure, it is transferred from the surfaces forming the coolant passage to the cooling air by means of a convective coefficient H_i . In the case of the element between stations 5 and 6 to which the secondary fin is attached, a fictitious convective coefficient H_f was used which represented the rate of heat transfer per unit area at the base of the fin and per unit temperature difference between the temperature at the base of the fin and the cooling-air temperature. This fictitious convective coefficient was expressed by the following equation

$$H_f = \frac{2 H_i \tanh \varphi_f L_f}{\tau_f \varphi_f}$$

where $\varphi_f = \sqrt{\frac{2 H_i}{k_f \tau_f}}$. The left-hand side of the elements from stations 3 to 7 shown in figure 3(b) represent the lines of symmetry across which no heat flows. The differential equation of heat-flow continuity was solved for each of the elements between stations 1 and 2, 2 and 3, 3 and 4, 4 and 5, 5 and 6, and 6 and 7. This resulted in a temperature distribution equation for each of the six elements and each equation contained two unknown arbitrary constants. The determination of the constants required the simultaneous solution of 12 equations which expressed the boundary conditions at the junction between the elements.

With the constants solved, the temperature at any point in the section could be expressed. A mathematical treatment of a similar one-dimensional heat-flow problem is given in reference 8. Temperatures were computed for stations 1 to 7 shown in figure 3(a) for a blade section with a mean spanwise geometry. The heat-transfer coefficient for the outside surface of the blade was determined from a heat-transfer correlation obtained in a static cascade for a similar profile. A correlation for heat transfer in tubes from reference 9 was used to evaluate average heat-transfer coefficients in the cooling-air passages.

The initial calculation used the specified cooling-air temperature at the blade base to determine the temperature distribution in the cross section at this station. Inasmuch as all the necessary conditions were then known at this station, the average or effective heat-transfer coefficient on the internal shell surface was readily determined from a simple heat-balance equation by assuming no spanwise heat flow. The nondimensional cooling-effectiveness parameter Φ was also calculated for stations 1 to 7 for later use in the analysis of spanwise temperature distribution. This procedure was carried out for three coolant flows in the range of interest.

One-dimensional spanwise temperature distribution. - A constant blade cross section, which is the mean section mentioned in the preceding section, was used to calculate the spanwise temperature variations for stations 1 to 7 shown in figure 3(a). The effective internal heat-transfer coefficient, evaluated as previously described, was applied in the cooling-air energy equation taken from reference 10 (equation (39)) to evaluate the spanwise variation of the cooling-air temperature for a specified, radial, effective gas temperature profile. The local values of Φ , determined according to methods described in the preceding section, for stations 1 to 7 were then used to determine the spanwise temperature distribution at these stations from the local effective gas and coolant temperatures.

Description of Equivalent Shell-Supported Blade Configuration

In order to determine to what extent the blade with an internal air-cooled supporting structure was an improvement over the more conventional shell-supported air-cooled blade, an analytical comparison was made for the two blades in the midchord region. In order to make a comparison, an air-cooled shell-supported-blade design was selected that was as similar as possible in internal geometry to that of the internally supported blade design. Inasmuch as the cross-sectional area of the supporting strut in the internally supported blade was tapered uniformly out to the $3/4$ span where the strut was discontinued except for the primary fins, which were continued to maintain structural rigidity to the tip, the cross-sectional area of the shell in the shell-supported

blade was assumed to decrease with the same uniform spanwise taper to the tip. The geometry of the base section of the shell-supported-blade design used for comparison is shown in figure 4. The thickness and spacing of the fins are identical with those in the internally supported blade (fig. 2). In the absence of an internal supporting structure, the fins are integral with both internal faces of the shell, thus breaking up the coolant passage into a number of spanwise passages with trapezoidal cross section. The following table compares the two configurations in terms of geometrical factors affecting the heat-transfer characteristics of the blade. The values given are for a mean spanwise geometry.

Geometry factor	Internally supported blade	Shell-supported blade
Summation of coolant-passage perimeter (in.)	9.66	8.686
Summation of coolant-passage flow area (sq in.)	0.1691	0.1985
Hydraulic diameter (in.)	0.0696	0.0914

Temperature Distribution Analysis in Shell-Supported Blade

The analysis of spanwise blade temperature distribution in the shell-supported blade was made according to methods given in reference 10. A one-dimensional spanwise solution was made directly by evaluating an effective inside heat-transfer coefficient that includes the influence of the internal finning. The analytical expression that permits consideration of fin dimensions, spacing, and thermal conductivity to determine an effective inside coefficient was modified to take into account the fact that two thicknesses of fins were used. However, their use had no influence on the comparison. This effective inside heat-transfer coefficient applies to the internal perimeter of the blade shell at the base of the fins and is related to the convective local heat-transfer coefficient at the surface of the fins. It was therefore unnecessary to make a separate analysis of the temperature distribution within the cross section as was the case with the internal-strut-supported blade configuration.

Conditions of Analysis

The analysis of the internal-strut-supported- and shell-supported-blade configurations was made for rated sea-level-static conditions in a J33 turbojet engine. The airfoil section at the root of the two air-cooled blade configurations was that of the standard turbine blade, but

the shell was nontwisted and similar to the experimental air-cooled blade reported in reference 2. At the rated engine speed of 11,500 rpm, the engine air flow was 72 pounds per second. The value of the profile heat-transfer coefficient for this condition was 0.0507 Btu/(sec)(sq ft)(°F), as determined from a static cascade heat-transfer correlation for this same profile. The spanwise effective gas-temperature profile, which is essentially the relative total temperature of the gas at the rotor inlet, was representative of that encountered in a previous experimental investigation and is given in figure 5(a). The temperature of the cooling air entering the cooling passages at the base of the blade was assumed to be 200° F. At the rated engine speed of 11,500 rpm, the blade tip speed is approximately 1325 feet per second at a diameter of 26 inches. The blade height used in the blade stress analysis was 4.0 inches. The temperatures in the load-carrying elements of the two configurations were compared for a range of coolant-flow ratios.

Comparison of Centrifugal Stress Distribution for the Two Configurations

Determination of the coolant flow required under engine operating conditions requires knowledge of the centrifugal stress in the load-carrying element and the allowable temperature of the blade metal. To obtain a valid comparison of the required coolant flow for the two configurations, the distribution of load-carrying metal should be as nearly the same as possible. The cross-sectional area of load-carrying metal was the same for the two designs up to the 3/4 span station where, in order to reduce the stress level in the base of the internal-strut-supported blade, the load-carrying member was discontinued except for the primary fins, which were continued to the tip inside the shell to maintain structural rigidity to the tip. It was obviously impossible to discontinue the load-carrying element at the 3/4 span of the shell-supported blade because the shell has an aerodynamic function to perform over the entire length of the blade. The stress distribution in the internal supporting strut was computed with the assumption that the thin shell was unable to support itself at the high temperatures and thus transmitted all of its weight in the centrifugal field to the internal supporting strut. For the shell-supported blade a similar assumption was made that the internal fins in the passage could not be attached to the blade root structure and therefore transmitted their weight to the shell. The spanwise centrifugal-stress distributions shown in figure 5(b) are very nearly the same for the two blades.

RESULTS AND DISCUSSION

Calculated temperature distribution in an internally supported blade. - The results of a temperature-distribution calculation for a coolant-flow ratio of 0.152 in the internally supported blade are shown in figure 6. The top curve is a plot of the spanwise variation of the effective gas temperature used in the calculation. The tendency of the spanwise-temperature distribution of the shell and the internal supporting strut to follow the general shape of the effective gas temperature profile is apparent. However, the shape of the spanwise cooling-air temperature curve reflects little influence of the midspan peak in the effective gas temperature profile. This characteristic of air-cooled blades has been observed in previous analyses (reference 10). It is also of interest to note that the peak temperature of the metal in the internal strut occurs at a larger radius than peak shell temperature. This may prove to be an advantageous feature of the internal-strut-supported blade since the maximum temperature is displaced toward a region of lower centrifugal stress. The hottest temperature on the shell for station 1 is about 1085° F at approximately 0.6 of the blade span from the root, whereas the highest temperature on the internal strut at stations 6 and 7 is about 805° F at 0.75 span.

The difference between the effective gas temperature and the shell temperature becomes a maximum at about the 0.3 span, where the shell temperature at station 1 is about 475° F below the effective gas temperature. The temperature difference of greatest interest is that between the shell and the internal supporting strut inasmuch as this type of blade is designed to insulate the load-carrying element from the hotter elements of the blade. The maximum temperature difference between the shell and the internal supporting strut also occurs at about the 0.3 span, where station 7 on the internal supporting strut is about 347° F cooler than station 1 on the shell. This temperature difference was from the hottest station on the shell to the coolest station on the internal supporting strut of the representative section. If the temperature at station 4 is selected to represent the mean chordwise temperature of the internal supporting strut and the arithmetic average of the temperatures at stations 1 and 2 is taken as the representative shell temperature, the temperature difference between the internal supporting strut and the shell is about 243° F for a coolant-flow ratio of 0.152.

The temperature difference between stations 2 and 3 is the calculated temperature drop in the spot welds between the shell and primary fins on the internal supporting strut. This temperature drop depends on the area of intimate thermal contact between the shell and the edge of the fins and thus on the number of spot welds and on the cross-sectional area of the nugget of the spot weld. It also depends on the thermal conductivity of the metal in the nugget and the heat-conduction path length through the nugget. Heat transfer from the shell to the fins

in the area between spot welds was neglected because it was reasoned that a dead air space would be formed when the hotter shell, tending to be longer than the internal supporting strut, buckled away slightly from the fins. The effects of radiation from the shell to the internal supporting strut were assumed to be insignificant and were therefore neglected.

The temperature drop from stations 3 to 4 in the primary fins is a function of the thermal conductivity of the metal, the convective heat-transfer coefficient from the side of the fin to the cooling-air, and the depth and thickness of the fins. The greater the depth-to-thickness ratio of the fins, the greater will be the temperature drop. However, there is a practical limit to this ratio in that the fins must be stout enough so that the shell can be attached by spot-welding or other means of attachment. The temperature drop from station 4 to 5, 6, and 7 is relatively small because of the large mass of metal through which the heat can flow. This relatively small temperature drop suggests that the secondary fins could possibly be eliminated from the design without much loss in cooling effectiveness.

A more general picture of the cooling characteristic of an internal-strut-supported blade is given in figure 7, where the average shell and strut temperatures are plotted for the 0.4 span station as a function of the coolant-flow ratio. The 0.4 spanwise station was chosen as a basis for comparison because it is the vicinity of tangency between an allowable spanwise temperature distribution curve and a blade temperature distribution calculated for a coolant flow selected so that tangency will occur. The effective gas temperature at this position is 1530°F . An arithmetic average of stations 1 and 2 in the cross section is considered to represent the chordwise average shell temperature, and the temperature at station 4 is considered to be the chordwise average strut temperature. As coolant-flow ratio increases, the difference between average shell and average strut temperature increases rapidly. At a coolant-flow ratio of only 0.01, a temperature difference of more than 200°F exists, which is very significant since the strut is well below 900°F under this condition. This indicates that a very large margin of strength can be maintained in the internal-strut-supported blade with nominal coolant flow.

Comparison of internally supported and equivalent shell-supported blades. - The advantage of the internal-strut-supported blade over the conventional configuration is brought out further in figure 8. At a coolant-flow ratio of 0.01 the internal-strut temperature is about 880°F , whereas the shell temperature of the shell-supported blade is about 1110°F . In order to achieve the same cooling effectiveness on the load-carrying element of the shell-supported blade as obtained at 0.01 coolant-flow ratio in the internal-strut-supported blade, almost 2.5 times the coolant flow is required. From the shape of the two curves it can be seen that the lower the desired temperature in either

configuration, the greater is the difference in required coolant flow. The advantage of the internally supported blade over the shell-supported blade increases as conditions become more severe.

Since the trends in gas turbine engines are toward higher gas temperatures and higher blade stresses, it is of interest to compare the limiting permissible stresses in the two configurations as coolant flow is varied. This is shown for the 0.4 span station in figure 9 for two effective gas temperatures using the stress-to-rupture properties of a noncritical metal, 17-22(A)S, for 1000-hour blade life as a basis of comparison. Comparison of the internal-strut- and shell-supported blades shows that the internal-strut-supported blade has considerably greater potentiality to withstand the increased stresses that may be anticipated in future engines. For an effective gas temperature of 1530° F at a coolant-flow ratio of 0.01, the allowable stress of the internal-strut-supported blade is about four times that of the conventional blade. The centrifugal stress at the 0.4 span is given by figure 5(b) as about 32,500 pounds per square inch. Thus the internal-strut-supported blade has a safety factor of over 2 for a coolant-flow ratio of 0.01 while the shell-supported blade does not have adequate strength to withstand the centrifugal load at that low coolant flow.

An important aspect of the substitution of cooled noncritical metals in turbine blades is the anticipated gain in maximum permissible stress relative to the commonly used high-temperature alloys. Design studies and analyses of future needs in turbojet engines, particularly where application of supersonic compressors is considered, have revealed the need for untapered turbine blades that can withstand centrifugal stresses approaching 100,000 pounds per square inch. It is expected that a highly effective convection-cooled shell-supported blade may go a long way in this direction, but the advantages of the internal-strut-supported blade become very significant when these severe conditions are imposed in the engine design. This advantage is illustrated by the two curves comparing the internal-strut- and shell-supported blades for an effective gas temperature of 1530° F. At a coolant-flow ratio of 0.01, the allowable stress for 1000 hours is approximately 75,000 pounds per square inch. For the shell-supported blade about 2.25 times the coolant flow of the internal-strut-supported blade would be required to achieve the same strength. The relationship shown by this curve is very significant because of the extremely high strength achieved with very small coolant flow. The influence on engine thrust and fuel consumption of coolant flows less than 1 percent of the gas flow is negligible according to analyses that have been made.

Under the more severe condition of higher gas temperature the advantage of the internal-strut-supported blade over the shell-supported blade is even greater as shown by the comparison for an effective gas temperature of 2530° F. For an allowable stress of 60,000 pounds per square inch the shell-supported blade requires more than 3.6 times as much

coolant flow as an internal-strut-supported blade. Increasing the effective gas temperature from 1530° to 2530° F increased the required coolant-flow ratio from 0.0065 to 0.0223 for an internal-strut-supported blade, while for the shell-supported blade it was increased from 0.015 to 0.0553.

For future engine designs having increased tip speed and blade height, a design stress approaching 80,000 pounds per square inch appears feasible where other characteristics of the blade metal are adequate. Although increased gas temperature would necessitate increased coolant-flow ratio, it appears that placing the load-carrying element of the blade within the coolant passage would permit the lowest coolant flow of any of the configurations that have been previously investigated. The air-cooled internal-strut-supported blade therefore appears to achieve a more nearly optimum integration of aerodynamic, cooling, and structural characteristics that would permit simultaneous increase in turbine-inlet temperature and engine specific mass flow per unit frontal area without sacrificing the basic simplicity of the air-cooling system as it has been applied in the past to the turbojet engine.

SUMMARY OF RESULTS

A new type of air-cooled blade design demonstrating a principle of submerging the load-carrying element as much as possible in cooling air within a thin high-temperature shell which is attached to the load-carrying element by means of spot welding was analytically evaluated and compared with a conventional type of shell-supported air-cooled blade. The following results were observed:

1. This new principle of blade design allowed the supporting structure or load-carrying element to be operated at considerably lower temperatures than the blade shell. These temperature differences increased with coolant flow. At a coolant-flow ratio of 0.01, this temperature difference was more than 200° F. More significant is the fact that for this relatively low coolant flow, the internal-strut temperature was well below 900° F and would therefore retain high strength.

2. Temperatures in the internal supporting strut were also considerably lower than in the shell of a comparable shell-supported blade. For a coolant-flow ratio of 0.01, the internal strut was more than 200° F cooler than the shell of a comparable shell-supported blade. This difference increased with coolant-flow ratio.

3. To achieve the same cooling effectiveness in the load-carrying element of a shell-supported blade as obtained at 0.01 coolant-flow ratio in the strut-supported blade required almost 2.5 times as much coolant flow. The lower the desired temperature in either configuration, the greater was the difference in required coolant flow.

4. Comparison of the internal-strut- and shell-supported blades showed that the internal-strut-supported blade has considerably greater potentiality to withstand the increased stresses that may be anticipated in future engines. Based on stress-to-rupture properties for 17-22A(S) for a 1000-hour blade life, the internal-strut-supported blade can be operated at a permissible stress of 75,000 pounds per square inch or about four times that of a comparable shell-supported blade with a coolant-flow ratio of 0.01 and an effective gas temperature of 1530° F. For an effective gas temperature of 2530° F, the internal-strut-supported blade required less than half as much coolant flow as the shell-supported blade to maintain a permissible stress of 60,000 pounds per square inch.

5. It appeared that placing the load-carrying element of the blade within the coolant passage will permit the lowest coolant flow of any of the convection-cooled configurations that have previously been investigated.

Lewis Flight Propulsion Laboratory
National Advisory Committee for Aeronautics
Cleveland, Ohio

REFERENCES

1. Ellerbrock, Herman H., and Schafer, Louis J., Jr.: Application of Blade Cooling to Gas Turbines. NACA RM E50A04, 1950.
2. Ellerbrock, Herman H., Jr., and Stepka, Francis S.: Experimental Investigation of Air-Cooled Turbine Blades in Turbojet Engine. I - Rotor Blades with 10 Tubes in Cooling-Air Passages. NACA RM E50I04, 1950.
3. Hickel, Robert O., and Ellerbrock, Herman H., Jr.: Experimental Investigation of Air-Cooled Turbine Blades in Turbojet Engine. II - Rotor Blades with 15 Fins in Cooling-Air Passages. NACA RM E50I14, 1950.

4. Stepka, Francis S., and Hickel, Robert O.: Experimental Investigation of Air-Cooled Turbine Blades in Turbojet Engine. IX - Evaluation of the Durability of Noncritical Rotor Blades in Engine Operation. NACA RM E51J10, 1951.
5. Schramm, Wilson B., Nachtigall, Alfred J., and Arne, Vernon L.: Preliminary Analysis of Effects of Air Cooling Turbine Blades on Turbojet-Engine Performance. NACA RM E50E22, 1950.
6. Arne, Vernon L., and Nachtigall, Alfred J.: Calculated Effects of Turbine Rotor-Blade Cooling-Air Flow, Altitude, and Compressor Bleed Point on Performance of a Turbojet Engine. NACA RM E51E24, 1951.
7. Livingood, John N. B., and Brown, W. Byron: Analysis of Spanwise Temperature Distribution in Three Types of Air-Cooled Turbine Blade. NACA Rep. 994, 1950. (Formerly NACA RM's E7B11e and E7G30.)
8. Livingood, John N. B., and Brown, W. Byron: Analysis of Temperature Distribution in Liquid-Cooled Turbine Blades. NACA TN 2321, 1951.
9. Lowdermilk, Warren H., and Grele, Milton D.: Influence of Tube-Entrance Configuration on Average Heat-Transfer Coefficients and Friction Factors for Air Flowing in an Inconel Tube. NACA RM E50E23, 1950.
10. Brown, W. Byron, and Rossbach, Richard J.: Numerical Solution of Equations for One-Dimensional Gas Flow in Rotating Coolant Passages. NACA RM E50E04, 1950.



NACA
C-28927

Figure 1. - Phantom view of internally supported blade.

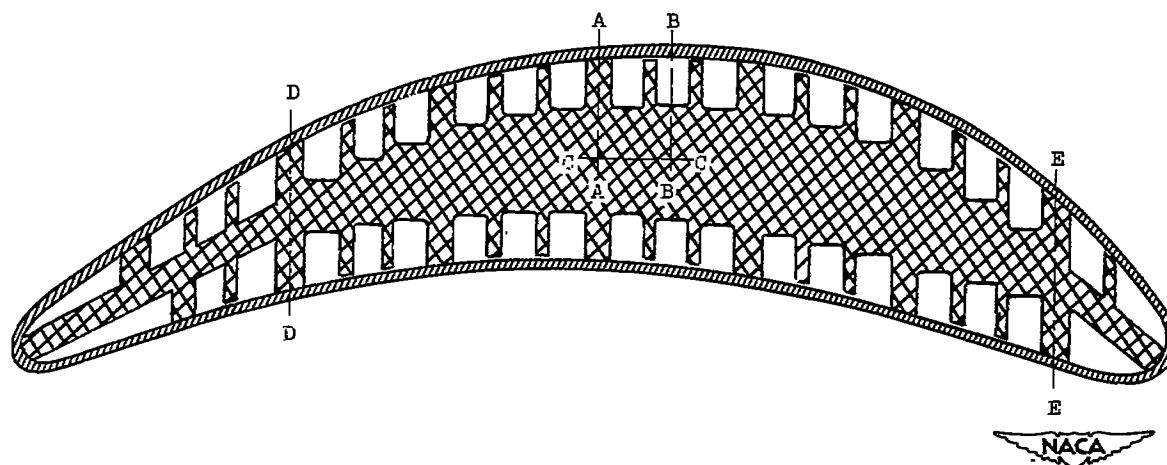
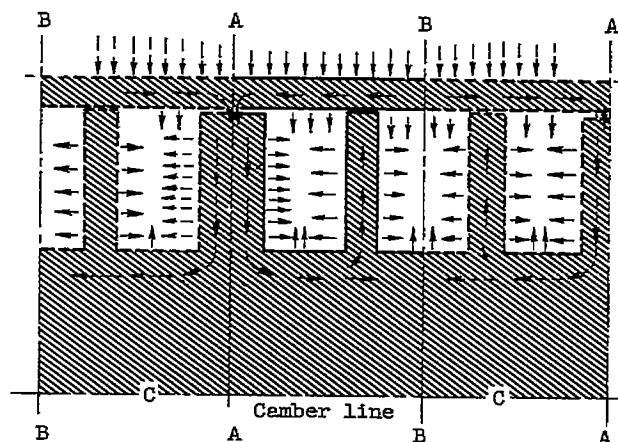
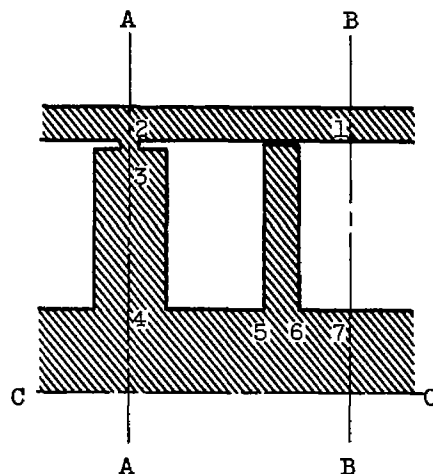
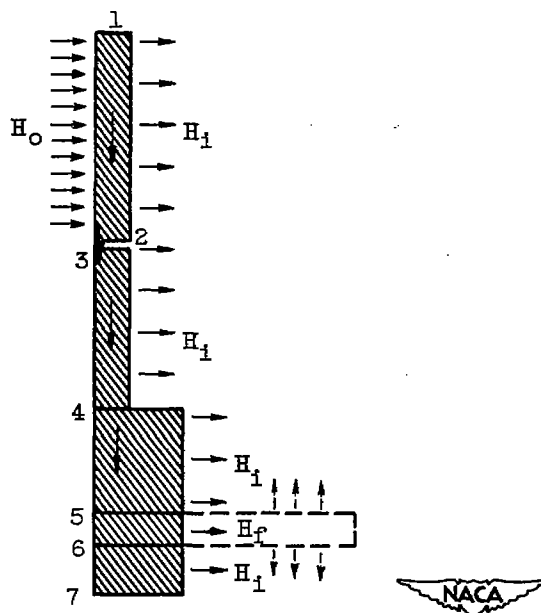


Figure 2. - Base section of internally supported blade design.



(a) Representative section from internally supported blade.



(b) Elements in representative section rearranged to permit solution as one-dimensional heat conduction. Convective coefficient, H_1 ; fictitious convective coefficient, H_p ; outside heat-transfer coefficient, H_0 .

Figure 3. - Schematic sketch of representative section from internally supported blade showing location of stations analyzed.

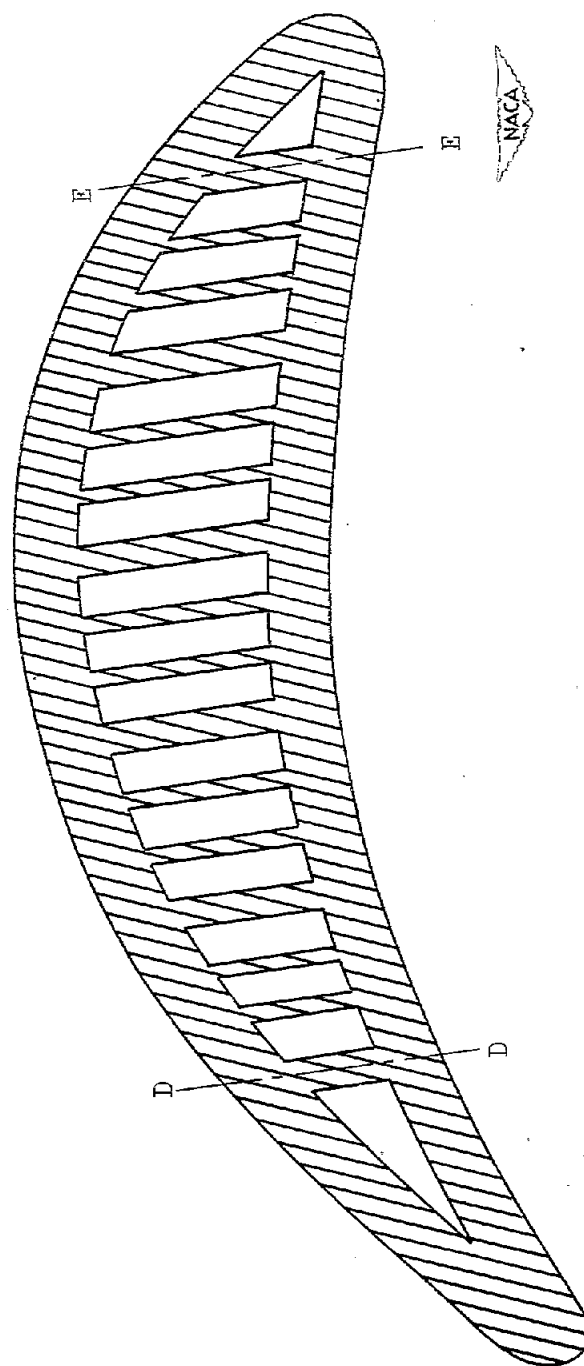
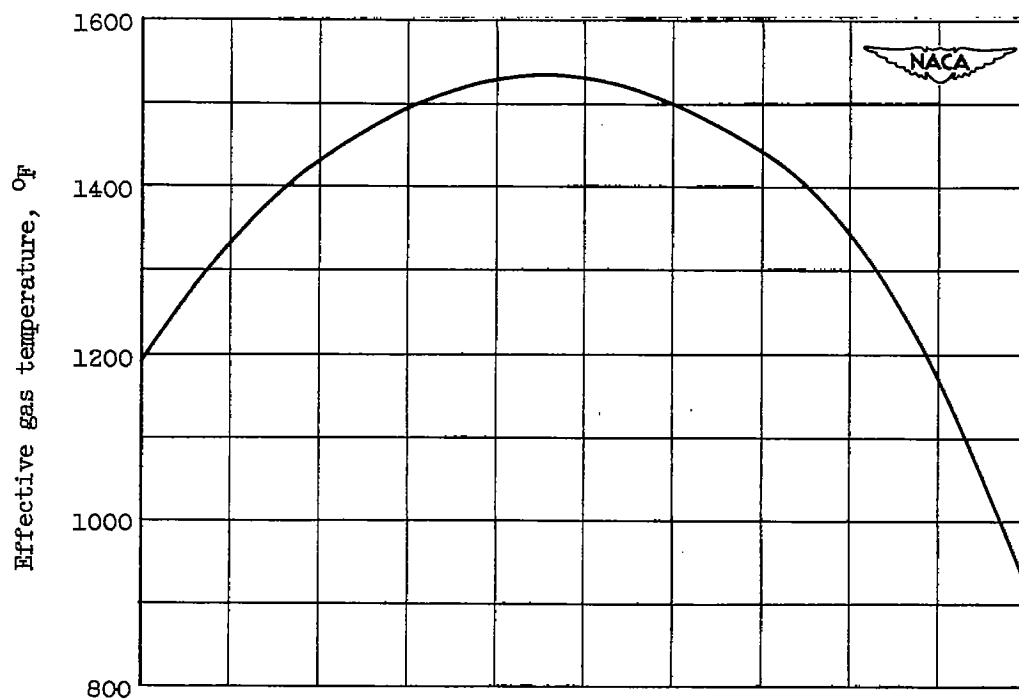
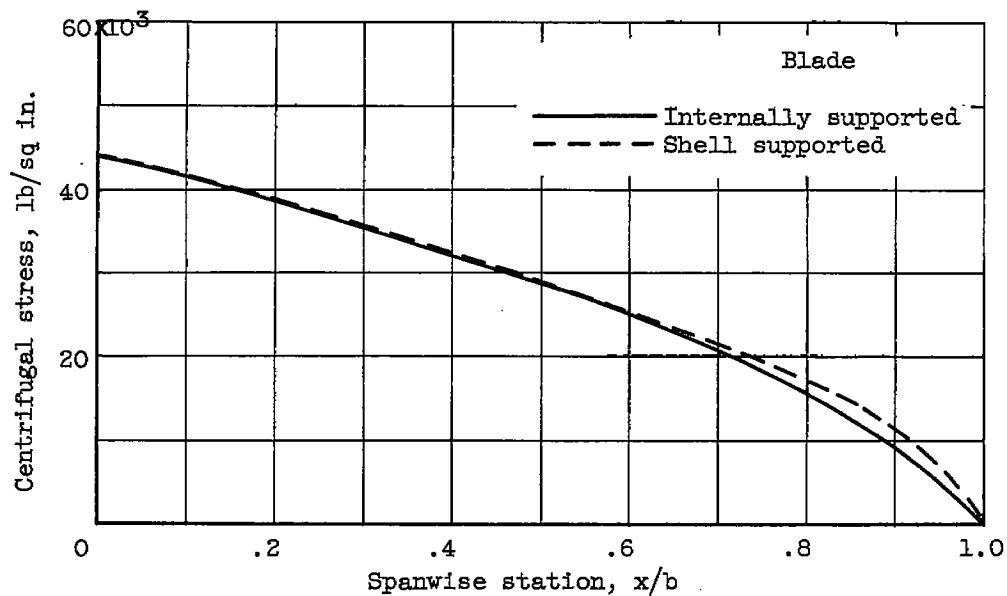


Figure 4. - Base section of shell-supported blade design used for comparison with internally supported blade of figure 2.



(a) Spanwise effective gas temperature profile.



(b) Spanwise centrifugal stress distribution.

Figure 5. - Spanwise effective gas temperature and centrifugal stress distributions used to compare internally supported blade configuration with shell-supported blade configuration.

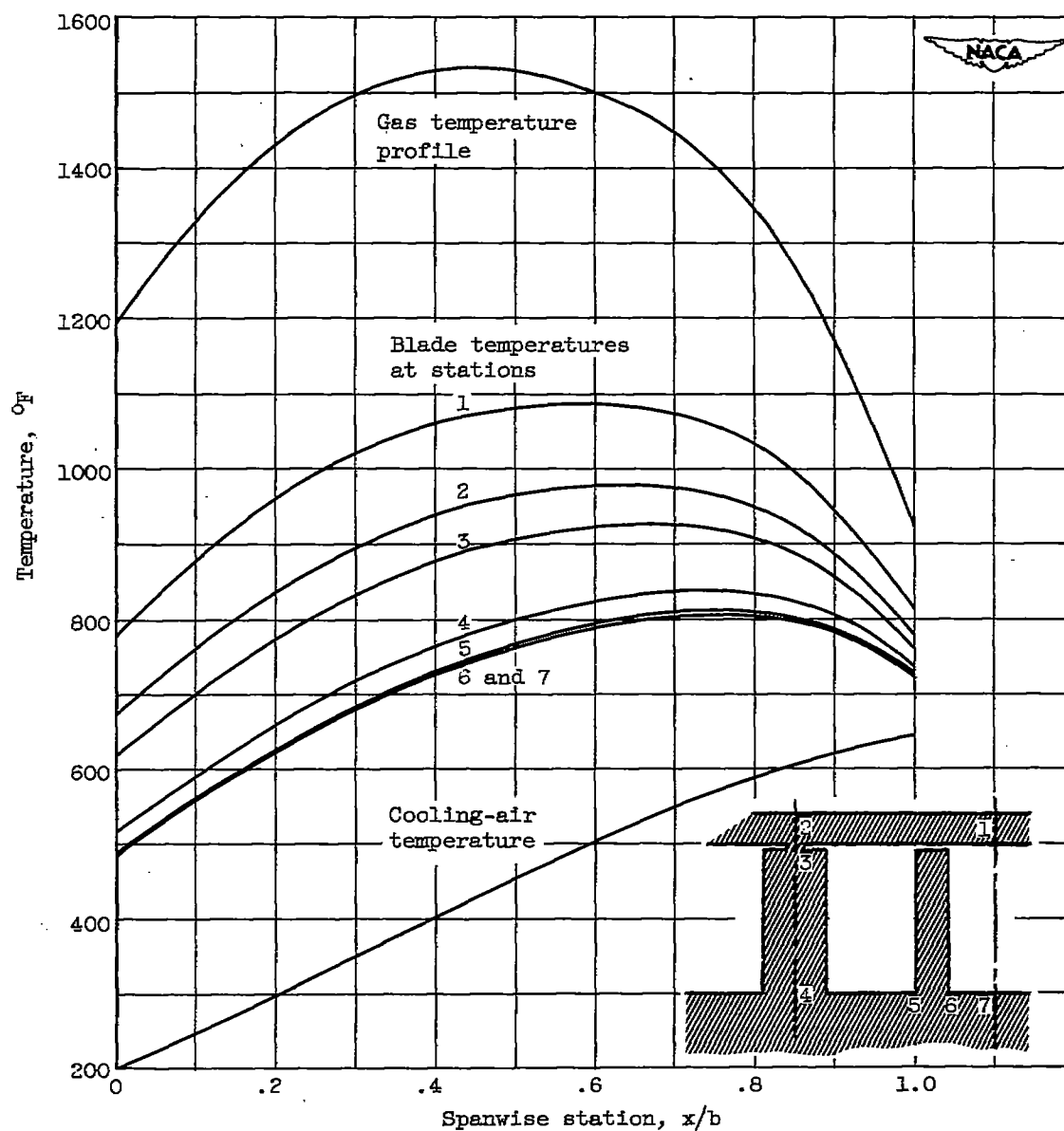


Figure 6. - Calculated temperature distribution in an internally supported blade for effective gas temperature profile shown. Coolant-flow ratio, 0.0152.

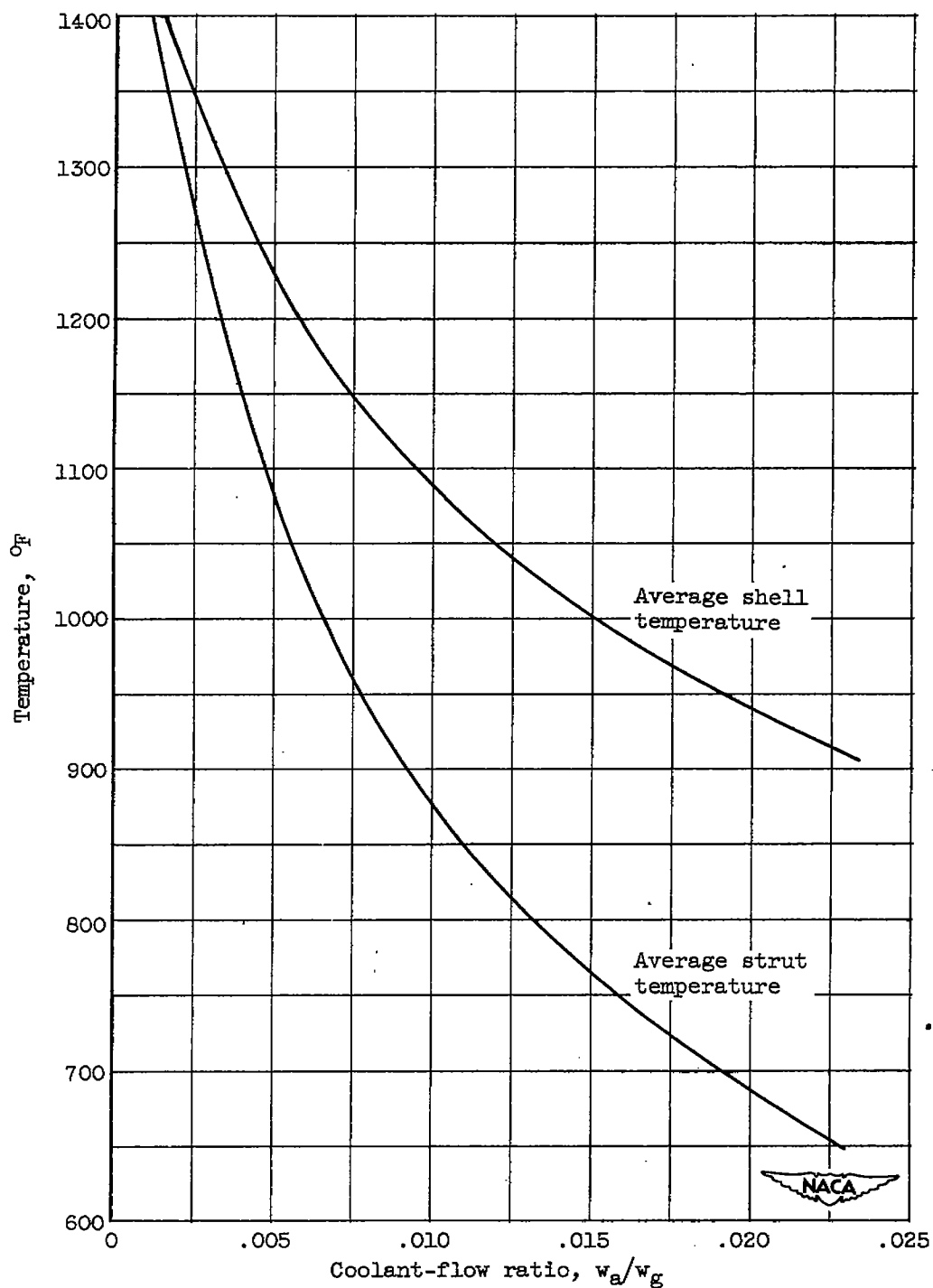


Figure 7. - Average shell temperature and average strut temperature against coolant-flow ratio for internally supported blade at 0.4 span. Effective gas temperature, 1530° F.

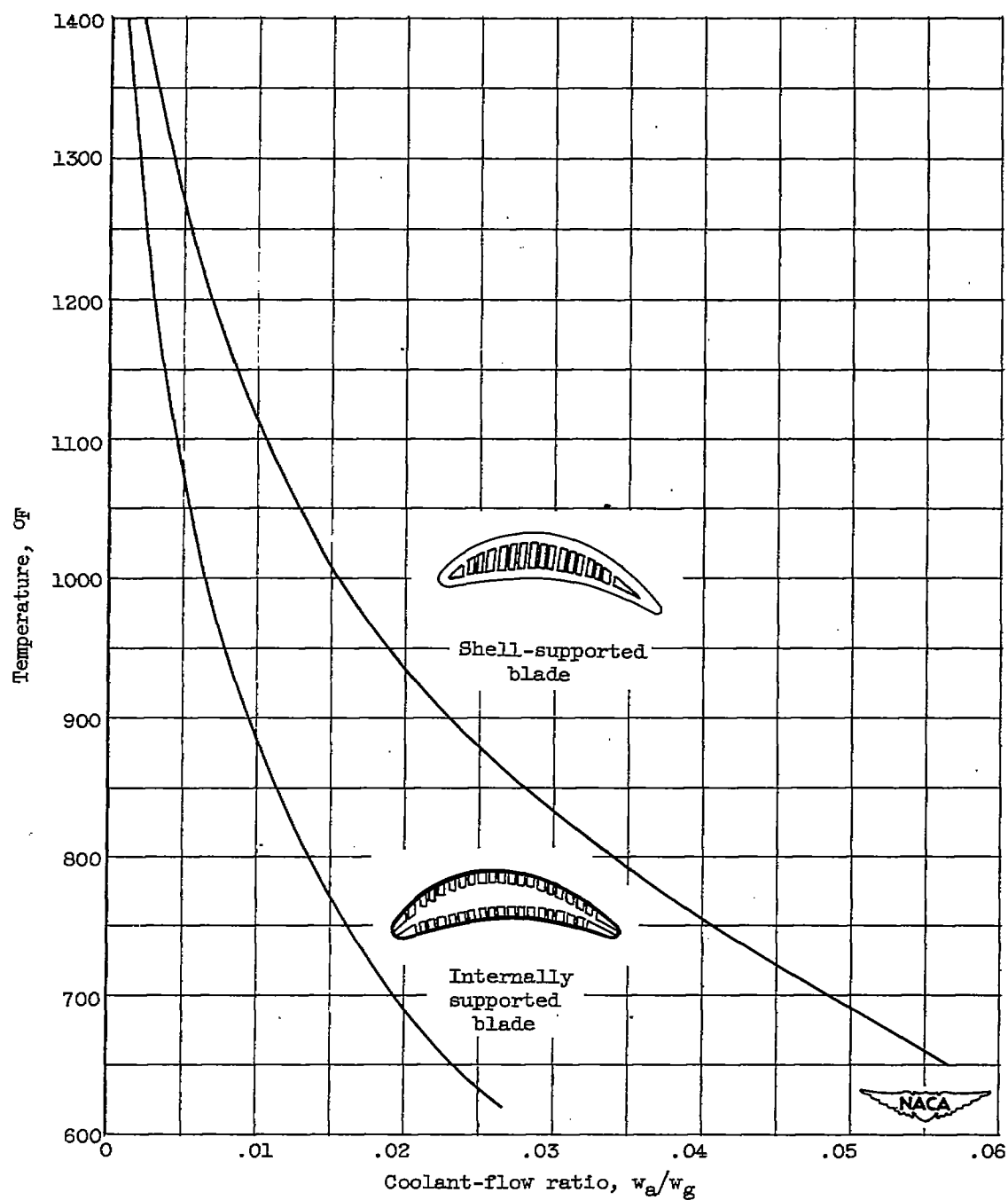


Figure 8. - Comparison of temperatures at 0.4 span in load-carrying elements of internally supported blade and shell-supported blade. Effective gas temperature, 1530° F.

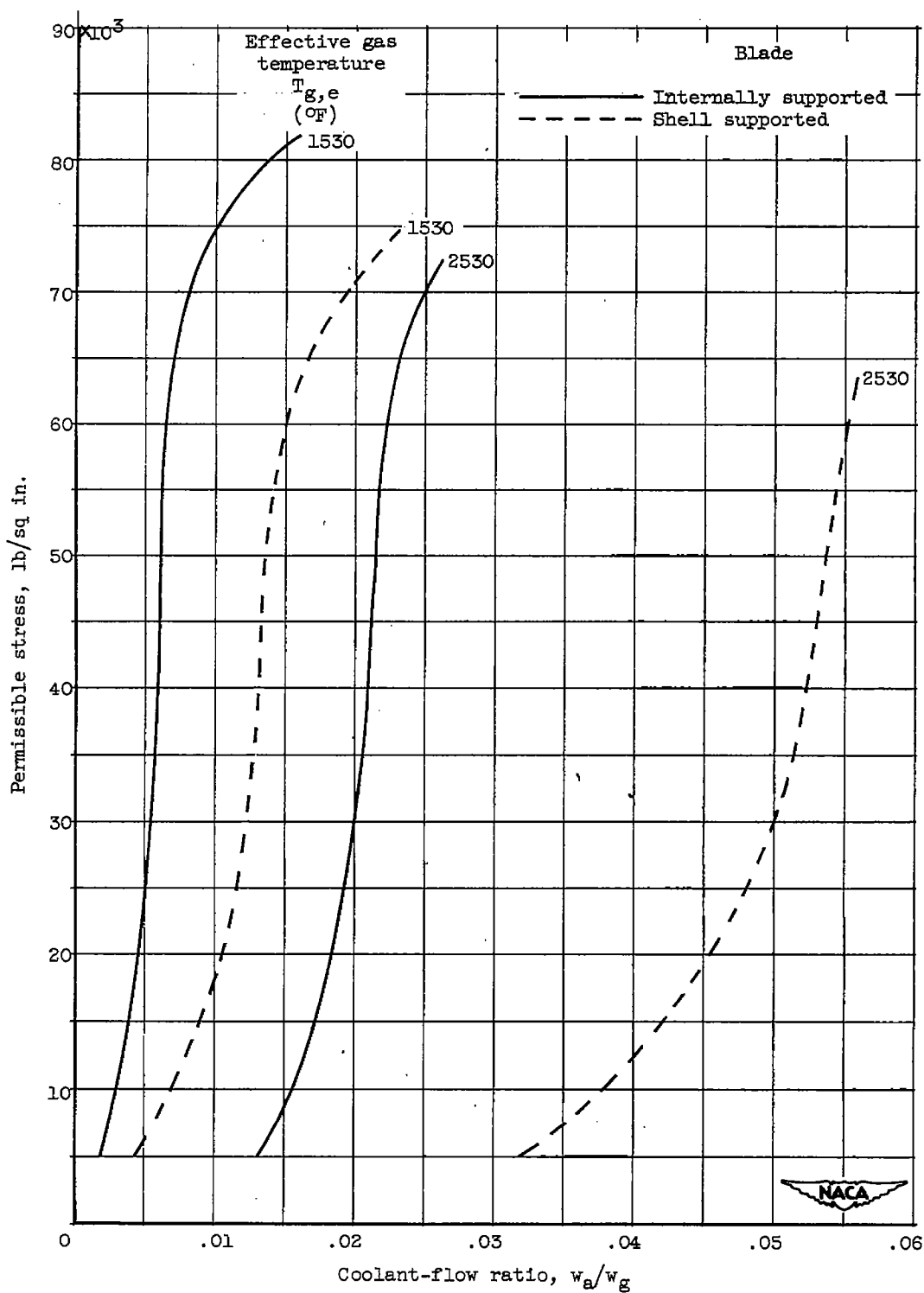


Figure 9. - Comparison of permissible stress at 0.4 span based on stress-to-rupture strength properties of 17-22A(S) for 1000-hour blade life.

NASA Technical Library



3 1176 01434 9824

